

The mechanism of pseudo-intercrystalline brittleness of precipitation-hardened alloys and tempered steels

ERHARD HORNBÖGEN

Ruhr-Universität Bochum, Bochum, West Germany

HEINRICH KREYE

Hochschule der Bundeswehr, Hamburg, West Germany

The term pseudo-intercrystalline brittleness is proposed to describe a fracture mechanism which can occur in poly-crystalline alloys which contain a fine dispersion of a second phase. If narrow particle-free zones develop along grain boundaries, separation can occur after large amounts of plastic strain, which is highly localized to the vicinity of grain boundaries. Since the hardened grain interior does not contribute to plastic deformation the total plastic deformation to fracture and fracture toughness remain small. Quantitative models are proposed to interpret the micromechanism of fracture and to describe the grain-size dependence of fracture toughness. The fracture of precipitation hardening aluminum alloys, creep resistant and structural steels are discussed in terms of the models. Finally an interpretation of the mechanism of stress-relief cracking in steel weldments is given.

1. Introduction

1.1. Two types of intercrystalline fracture

Intercrystalline embrittlement is usually associated with cleavage along the plane of grain boundaries or interphases. This mechanism is favoured by film-like brittle precipitates or by segregation of certain alloying elements into the plane of the boundary. These elements are thought to either locally weaken the bond strength or reduce the possibilities of plastic relaxation of the boundary, which may be exposed to a stress concentration, for example, by dislocations piled-up from inside the grain. Most investigations of intercrystalline embrittlement of this type are therefore concerned with the identification of harmful trace elements and their kinetics of segregation to boundaries [1]. Sometimes confused with this well-known mechanism is a different one which is predominantly caused by extreme, but highly localized ductility in the vicinity of grain boundaries. It was first observed in Al-Zn-Mg alloys that cracks initiated at so-called super-bands, i.e. slip steps

which are much higher than the usual transcrystalline steps [2]. The fracture surfaces of several precipitation hardening alloys showed an intercrystalline appearance, especially if they were aged close to peak hardness [3, 4]. A more subtle microscopic investigation indicated, however, that separation had not occurred directly at the grain boundary, but after high deformation in a particle-free zone (PFZ) of a diameter of about 10 to 100 nm [3-5]. In some cases this zone is so narrow that it is difficult to detect it even by electron microscopy. Based on this observation, theoretical models were developed which correlate the fracture toughness of precipitation hardened aluminium alloys at room temperature with important microstructural features [6, 7]. Experiments on the temperature dependence of microplasticity indicated that the inhomogeneity of plastic deformation was reduced towards lower temperature due to increasing work hardening inside the PFZ. Based on this observation, similar phenomena could be expected in iron-base alloys with cor-

responding microstructures in a temperature range around 200° C and above ($T > 0.25 T_M$, where T_M is the melting point). A large number of observations on fracture under creep conditions and in heat-affected zones of weldings indicated that this type of intercrystalline brittleness is not restricted to aluminium alloys but is a general phenomenon. It occurs in particle-containing steels such as HSLA steels, creep resistant steels, tempered tool steels, precipitation hardened austenitic steels and high nickel alloys after certain heat treatments and in a temperature range down to room temperature [8–12].

An additional type of pseudo-intercrystalline cracking was observed at very low temperatures in ferritic alloys containing copper particles. Cleavage along the {100} plane occurred which again was restricted to the PFZ. This preferred brittleness of the PFZ is due to the fact that particles impede transcrystalline crack propagation [13].

1.2. Two types of particle-free zones (PFZ)

Particle-free zones have attracted the attention of those concerned with solid-state nucleation since the advent of transmission electron microscopy [14–21]. As this theme has been treated again recently [21], only the features which are important for this discussion will be mentioned here.

A PFZ can be due to solute depletion and due to vacancy depletion in the environment of high-angle grain boundaries. Vacancy depletion is caused by diffusion to and annihilation at grain boundaries of supersaturated vacancies. This usually occurs during quenching from a temperature at which a higher vacancy content is present in thermodynamic equilibrium. The additional

requirement for the formation of a PFZ is that nucleation of particles inside the grains is favoured at the sites in which single vacancies or vacancy clusters exist. This is usually the case for precipitate phases with a larger specific volume than the matrix (for example in Al–Zn–Mg alloys, but not in Al–Cu–alloys) [20]. Inside the vacancy gradient at the grain boundary, nucleation conditions become less favourable and therefore the density of particles decreases. The diameter of the PFZ, ($d_{PFZ} = d_\beta$) decreases with increasing quenching rate and it increases with increasing effectiveness of vacancies to catalyse general nucleation in the matrix.

The second mechanism for the formation of a PFZ is even more commonly observed. It requires a precipitation system in which the most stable phase is incoherent with the matrix and therefore preferably forms at grain boundaries. These grain-boundary precipitates act as solute sinks in the environment of grain boundaries. General nucleation is inhibited due to the local decrease of supersaturation. As a consequence, a narrow PFZ surrounds a grain boundary at both sides after relatively large incoherent particles had formed directly at the boundary [22]. Therefore the zone as a whole is not “particle-free” in a strict sense. The matrix is usually purified and locally softened to a large degree as a consequence of attainment of local equilibrium close to the matrix–particle interface. In the direct neighbourhood of a PFZ of the first type the composition of the original supersaturated solid solution may be preserved because no nucleation of particles is necessarily required. Therefore solid solution hardening is still effective while particle hardening is absent [7], (Figs 1 and 2).

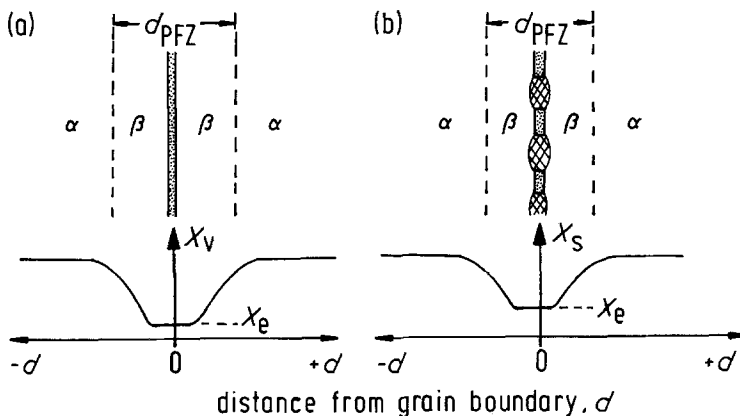


Figure 1 Schematic representation of particle-free zones (PFZ), showing (a) vacancy depletion and (b) solute depletion (x_s = solute content x_v = vacancy content).

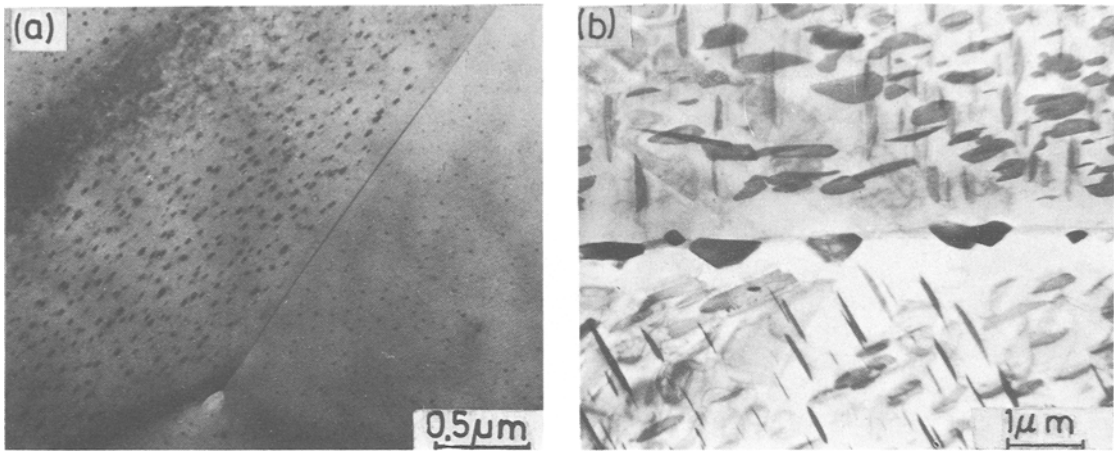


Figure 2 TEM micrographs of PFZs (a) α -Fe + 1 wt% Cu, (b) Al + 3 wt% Cu, homogenized for 16 min at 300° C.

2. Experimental observation

2.1. Initiation and propagation of cracks in precipitation hardened aluminium alloys

Al–Zn–Mg alloys predominantly form PFZs of Type I (vacancy depleted), while Al–Cu alloys form Type II because of the smaller size of Cu atoms as compared to Al (Fig. 2). Most experimental investigations were conducted with alloys of the Al–Zn–Mg type around ambient temperature. Fig. 3a shows the results of a bending test by which the critical strains for crack initiation can be measured using a gauge grid. In addition, information on the particular sites of crack initiation is obtained from light-microscopy or scanning electron microscopy of the originally polished surface (Fig. 3b, c). As the deformation at fracture decreases in the aged condition, crack initiation shifts from transcrystalline to intercrystalline. The term “superband” is used for the large steps that appear in the surface before cracks start to form. Superbands disappear again in the overaged condition. Results of measurements of fracture toughness, K_{Ic} , are shown in Fig. 4. For the peak aged condition, crack propagation energy K_{Ic} or G_c decreases with increasing grain size, while the yield stress is almost independent of the grain size [5]. The microscopic investigation of the crack path indicates that minor transcrystalline portions occur, if the plane of a grain boundary differs by more than 80° from the normal crack direction. For the solid solution and the overaged alloy this critical angle decreases to almost zero [23]. The microscopic investigations showed that the PFZ in Al–Zn–Mg was usually not of pure Type I

nature. It occasionally contained non-coherent particles which aided intercrystalline separation by formation of pores [22] (see Fig. 5).

2.2. Crack formation in structural and heat-resistant ferritic steels at elevated and ambient temperature

In a variety of steels including plain carbon, low alloy and high alloy steels PFZs of Type II (solute depleted) can occur. When the steel is transformed to martensite or the lower bainite and subsequently annealed, carbon atoms move from former austenite grain boundaries to adjacent martensite lath interfaces. In addition carbide particles, nucleated preferably at the former austenite grain boundaries, acts as sinks for carbon atoms. The resulting microstructure is then characterized by a particle-free or particle-denuded zone along former austenite grain boundaries or by relatively large carbides at former austenite grain boundaries with a PFZ to both sides, as demonstrated in Fig. 6.

In the case of C and C–Mn steels, PFZs seem to have no detrimental effect on the mechanical behaviour. During plastic deformation yielding can be expected to start within the mechanically soft PFZ, but proceeds in a more homogeneous way. However, if the strength of the grain interior is substantially increased by a fine dispersion of alloy carbides of Mo, Cr, V, Nb and/or Ti, yielding may become strongly limited to PFZs resulting in a pseudo-intercrystalline cracking after low total elongation. In practice, this type of cracking has been observed in heat-resistant steels operated under load at elevated temperature [10, 24] and in highly restrained components of high-strength

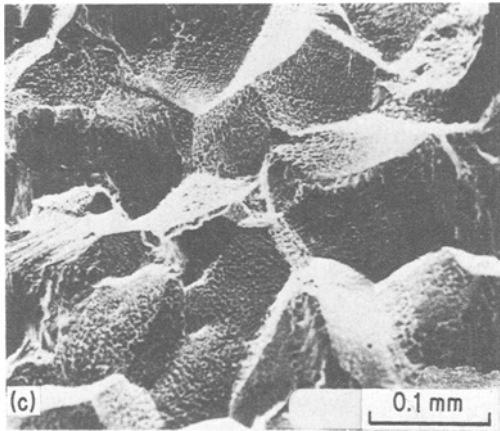
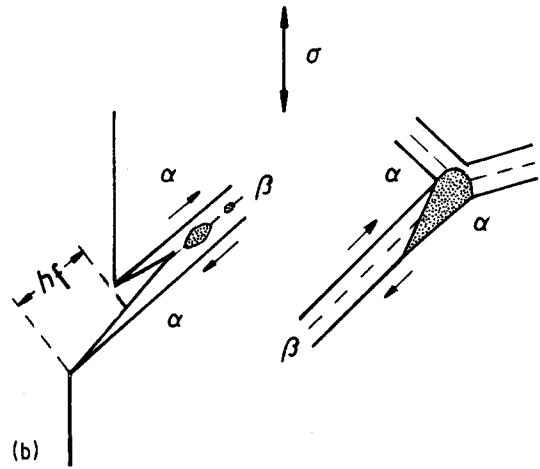
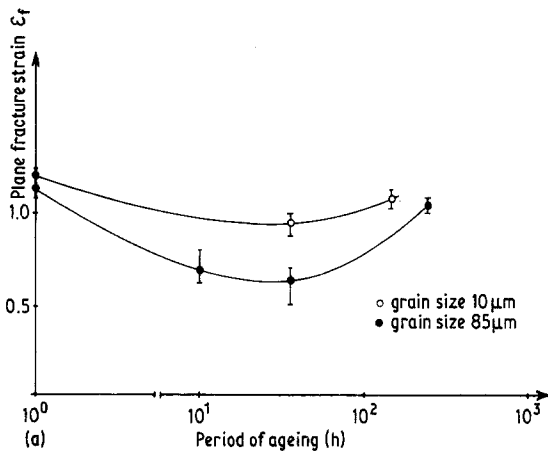


Figure 3 Fracture due to localized plastic deformation in precipitation hardened Al-4.6 wt% Zn-1.2 wt% Mg showing (a) fracture strain, ϵ_f , as a function of grain size and ageing time (b) crack initiation at a superband in the surface or at a grain boundary junction in the interior (c) typical dimpled pseudo-intercrystalline fracture surface.

steels heat-treated for stress relieving [8, 10]. In both instances deformation occurs at high temperatures and low strain rates. After extended deformation of the PFZ, cracks have been observed to start at triple points of former austenite grain

boundaries (Fig. 3b) or at large carbide particles and then propagate along PFZ. As deformation temperature decreases, the fracture mode changes from intercrystalline to transcrystalline. At ambient temperature localized yielding restricted to the PFZ can still be found in the beginning of plastic deformation, but fracture occurs almost completely in the transcrystalline mode [23]. This can be explained by an increasing effect of work hardening in the PFZ.

2.3. Stress-relief cracking in the heat-affected zone of steel weldments

The term stress-relief cracking (SRC) refers to the intergranular cracks that develop in the heat-affected zone of welded assemblies during a post-weld heat-treatment. According to the welding specification for heavier sections of high-strength steels, a post-weld heat-treatment is required to reduce residual stresses and enhance toughness. Stress-relief is then accomplished by a creep process in which elastic strain is converted to plastic strain. Therefore it is necessary to heat the welded joint to a temperature where creep can take place. The susceptibility to crack formation during such a heat-treatment is dependent upon alloy composition, welding conditions and stress-relieving cycle [9, 10, 24-32]. SRC has been observed in a number of low-alloy structural steels and heat-resistant steels. Steels containing critical amounts

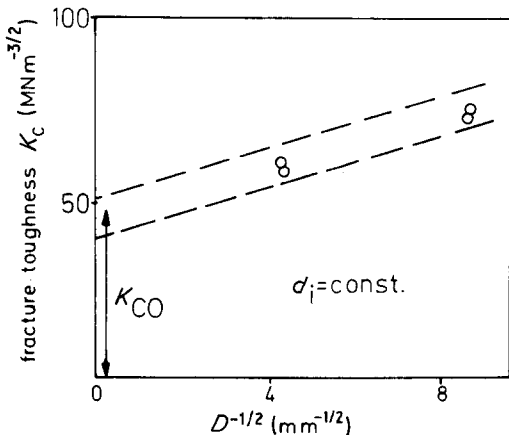


Figure 4 Grain-size dependence of fracture toughness in Al-4.6 wt% Zn-1.2 wt% Mg.

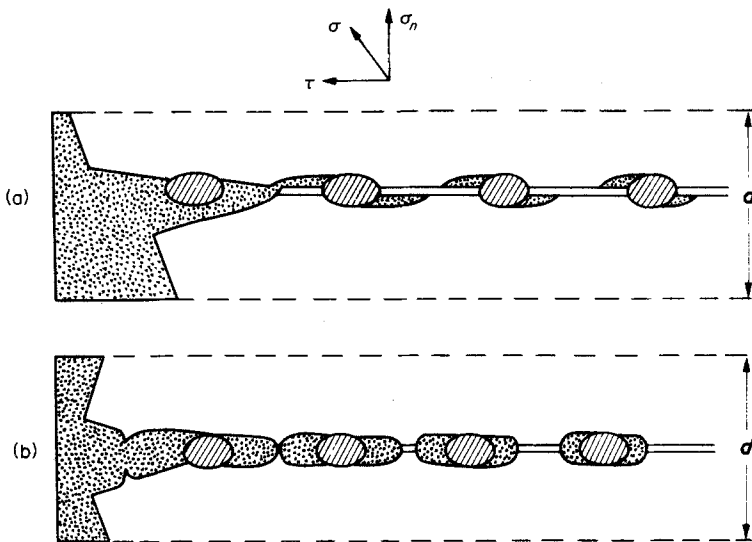


Figure 5 The mechanism of separation in the PFZ by pore formation at a non-coherent particle caused by (a) a shear stress, τ , (b) tensile stress, σ .

of Mo, Cr, V, Nb and/or Ti are particularly sensitive to SRC [9, 10]. There is some indication that trace elements like Sn, P, Cu and Sb may be harmful, too [30, 34]: The tendency towards cracking increases with the presence of high stresses and local stress concentrations, (e.g., in highly restrained structures, heavy sections, high-energy welding techniques and heavy thermal cycling).

Cracking occurs in the coarse grained area of the heat-affected zone along former austenite grain boundaries. Formation and propagation of cracks must be associated with a highly localized deformation of the vicinity of these boundaries. The intergranular fracture shows small dimples surrounded by ductile torn ridges (Fig. 7a, b). At grain boundaries plastic offsets of up to $5 \mu\text{m}$ have

been measured in front of the crack tip (Fig. 7c) [31]. A variety of tests have been introduced to study the susceptibility of a steel to SRC [9, 33]. Notched stress-rupture tests on weld-simulated samples of various creep-resistant and HSLA steels have been used to determine a relationship between stress-relieving temperature and time to failure. A C-shaped curve was obtained with the shortest time to fracture at a temperature between 580 and 640°C [9].

3. Discussion

3.1. Pre-requisites for inhomogeneous plastic strains

The micromechanical situation at which pseudo-intercrystalline cracking is observed is characterized

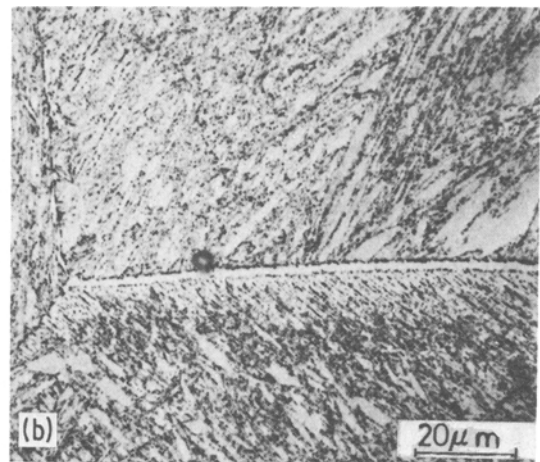
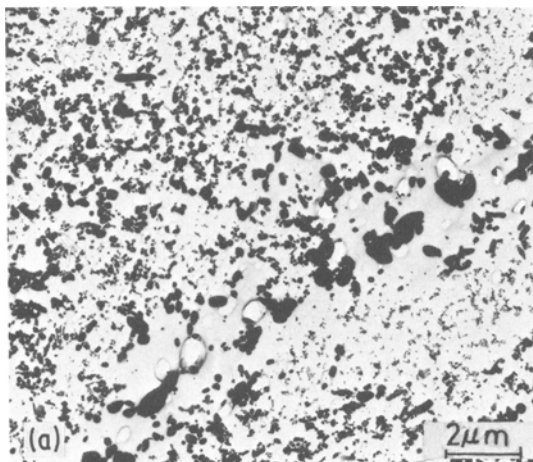


Figure 6 Former austenite grain boundary in HSLA steel after 3 min at $1300^\circ\text{C}/\text{H}_2\text{O}$ + 3 h 600°C showing large carbides at former austenite grain boundaries with PFZ on both sides. (Replica).

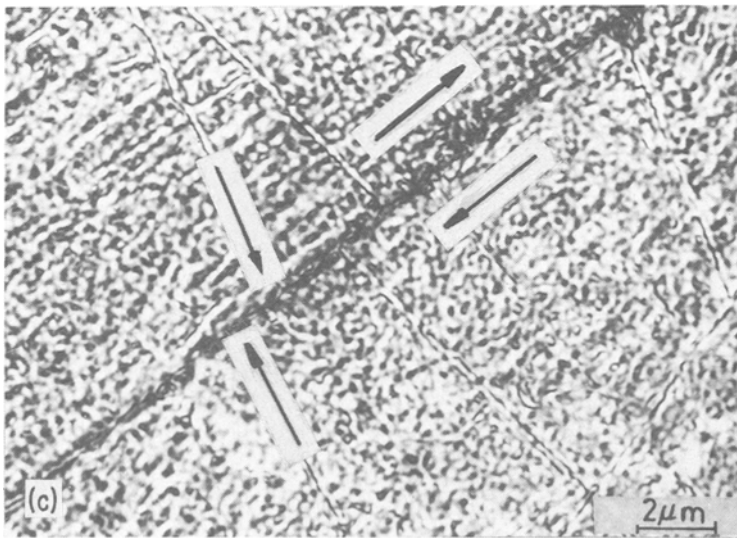
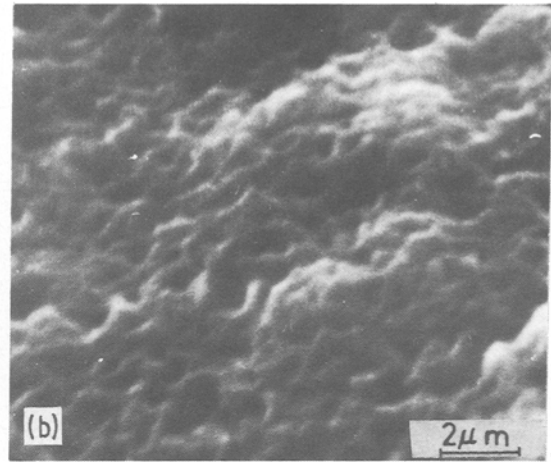
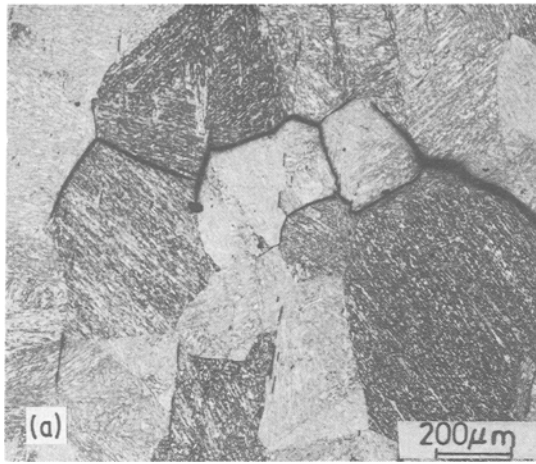


Figure 7 Microstructural features of stress-relief cracking in the steel 22NiMoCr37. Weld simulated heat-treated 10' 1300° C/ H₂O and strain annealed at 620° C showing (a) intergranular crack, (b) dimpled microstructure of the grain surface after cracking and (c) offset of former austenite grain boundaries in front of the crack tip.

by a precipitation hardened interior of grains, α , surrounded by a net of soft material, $\beta = \text{PFZ}$, (see Fig. 8a). During an ageing sequence the mechanical properties of α and β are differentiated by hardening of α and quick softening of β . At the peak aged condition the partial tensile properties can be principally characterized as shown in Fig. 8b, c. Exposed to an uniaxial stress, the strain in α and β , $\bar{\epsilon}_\alpha$ and $\bar{\epsilon}_\beta$, must be different while the stress is constant. The total strain, ϵ , depends on the volume portions f_α and f_β , i.e.,

$$\epsilon = \bar{\epsilon}_\alpha f_\alpha + \bar{\epsilon}_\beta f_\beta. \quad (1)$$

If plastic deformation only is considered and β ruptures before α yields (Fig. 8c), Equation 1 can be reduced to

$$\epsilon = \bar{\epsilon}_\beta f_\beta, \quad (2a)$$

for

$$\bar{\sigma}_{f\beta} < \bar{\sigma}_{y\alpha}, \quad (2b)$$

where $\bar{\sigma}_{f\beta}$ is the fracture strength of the PFZ and $\bar{\sigma}_{y\alpha}$ is the yield strength of the grain interior.

If the mechanical properties of α and β approach each other during overageing, transitional relations between Equations 1 and 2 will have to be applied [23].

3.2. Crack initiation and propagation in alloys with plastic strain restricted to particle-free zones

If deformation takes place exclusively in the PFZ, β , crack initiation in bending and elongation at fracture is determined by its ductility, $\bar{\epsilon}_{f\beta}$ where the total fracture strain ϵ_f is defined by

$$\epsilon_f = \bar{\epsilon}_{f\beta} f_\beta \approx \bar{\epsilon}_{f\beta} \frac{d_\beta}{D}, \quad (3)$$

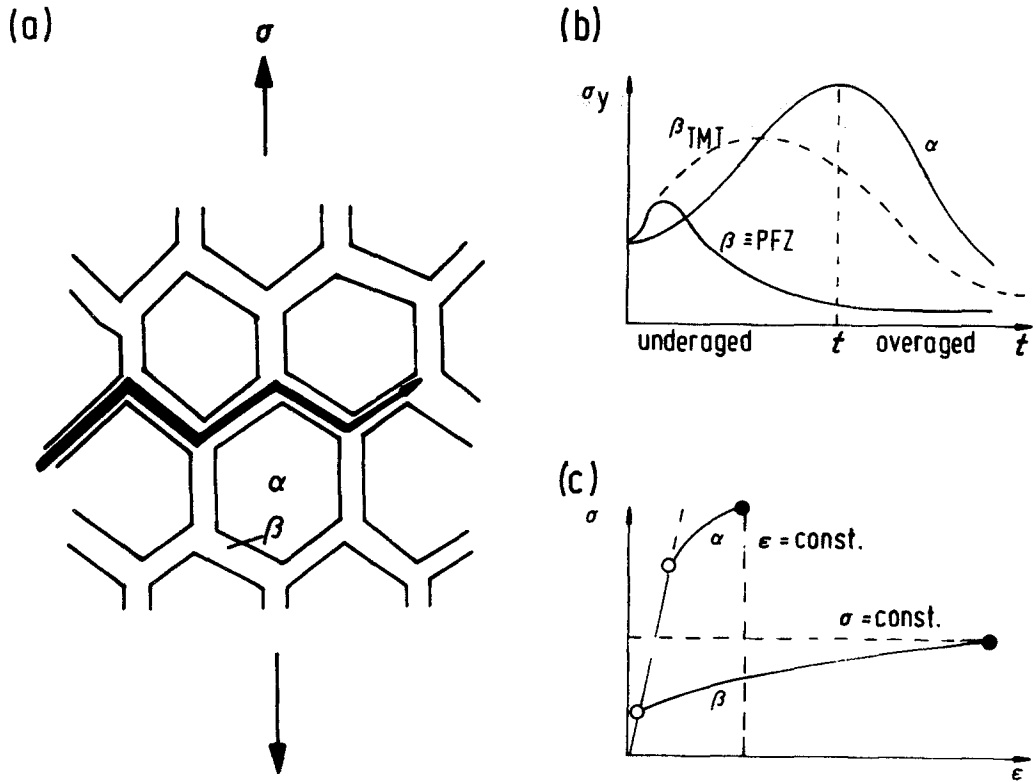


Figure 8 Micromechanical behaviour of alloys containing a net of PFZs. (a) crack propagation along the PFZs, β , (b) the change of the partial properties of α and β during an ageing sequence (β_{TMT} represents the yield strength of the PFZ modified by a thermomechanical treatment) (c) partial stress strain curves of the microstructural components in the peak-aged condition.

where d_β is the diameter of the PFZ, D is the grain size, and $D \gg d_\beta$. The critical step height, h_f , of a superband at which a crack can start in the surface is (see Fig. 3b)

$$h_f = \bar{\epsilon}_{f\beta} d_\beta. \quad (4)$$

Deformation at fracture will decrease with increasing grain size if the properties and dimension of the PFZ remain constant. For the deformability, $\epsilon_{f\beta}$, of the particle-free zone, β , the same criteria apply as for bulk material. The local volume-fraction of non-coherent particles, which is usually high, will reduce local ductility due to enhanced pore formation [22] (see Fig. 5).

For a quantitative treatment of crack propagation it is useful to consider the ratio of microstructural and fracture mechanical dimension. For $r_p > D$, where r_p is the radius of the plastic zone, the plastic zone covers one or more grains. Energy, however, is dissipated only in the volume-fraction, f_β , of the PFZ. From this a relationship follows for the total crack extension energy G_{Ic}

or for the fracture toughness K_{Ic} (see Fig. 9)

$$G_{\text{Ic}} = \frac{K_{\text{Ic}}^2}{(1-\nu)E} = \bar{G}_{\text{Ic}\beta} f_\beta = \bar{G}_{\text{Ic}\beta} \frac{d_\beta}{D}, \quad (5)$$

where ν is Poisson's ratio or, if the grain-size dependence of the fracture toughness is expressed by a relationship similar to that for the grain-size dependence of the yield stress (Fig. 4):

$$K_{\text{Ic}} = K_{\text{Ic}0} + \frac{C}{\sqrt{D}}. \quad (6)$$

C contains all the constant properties of the microstructure except the grain size D . If a crack path is not limited to the PFZ but moves straight through both microstructural components, the rule of mixtures should be applicable (compare Equation 3). In this case a much higher toughness will be expected because the complete volume of the material contributes to the dissipation of energy:

$$G_{\text{Ic}} = \bar{G}_{\text{Ic}\alpha} f_\alpha + \bar{G}_{\text{Ic}\beta} f_\beta \quad (7)$$

Equation 5 is a special case of Equation 7.

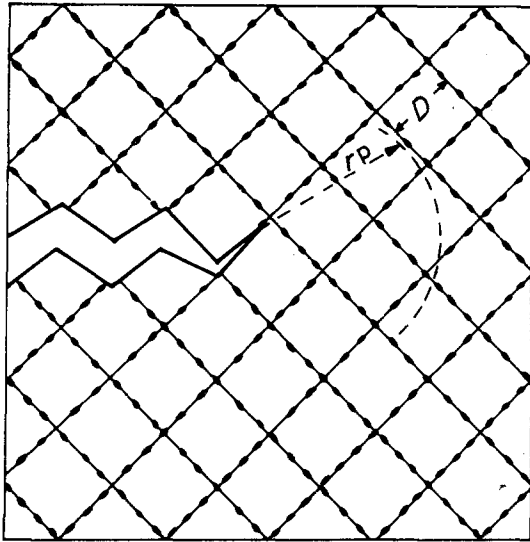


Figure 9 Schematic representation of the ratio of plastic zone radius, r_p , and grain diameter, D .

K_{Ic0} is the minimum fracture toughness which can be measured by pseudo-intercrystalline separation of a bi-crystal.

3.3. The mechanism of stress relief cracking

The microstructural situation which develops in the heat-affected zone during welding and stress-relief heat-treatment is characterized by a net of soft material with a highly strengthened interior as described schematically in Fig. 8. During the welding cycle the area close to the weld metal is quickly heated to a peak temperature of about 1250 to 1400° C at which the austenite grains grow considerably and alloy carbides become partly or completely dissolved. Upon cooling the austenite transforms to the martensite or the lower

bainite. The subsequent stress-relieving heat-treatment leads to the formation of PFZs along prior austenite grain boundaries, while simultaneously the interior of the grains becomes further strengthened by a fine dispersion of newly formed alloy carbides (see Fig. 8b). Such carbides cannot form in the carbon depleted PFZ. Therefore the yield strength of the PFZ ($\bar{\sigma}_{y\beta}$) decreases continuously, while the yield strength of the grain interior ($\bar{\sigma}_{y\alpha}$) increases and exhibits a maximum. The deformation process during stress-relieving heat-treatment is described in Fig. 10a. As $\bar{\sigma}_{y\beta}$ falls below the level of the internal stress, σ_i , plastic deformation occurs within the PFZ (β). σ_i cannot be reduced sufficiently through a highly localized deformation mode because the amount of total deformation remains small (Equation 2). As deformation proceeds, stress concentrations build up at triple points of former austenite grain boundaries and at relatively large grain boundary carbides. Since the concentrated stress cannot be reduced by plastic deformation of grain interior ($\bar{\sigma}_{f\beta} < \bar{\sigma}_{y\alpha}$), crack formation becomes inevitable.

A different situation exists in plain carbon steels where SRC does not occur (see Fig. 10b). Again, PFZs do form during welding and stress-relief heat-treatment, but the grain interior is not strengthened by alloy carbides. With $\sigma_{f\beta} > \sigma_{y\alpha}$ stress concentration within the PFZ can induce plastic deformation of the grain interior. The total strain achieved by this combined deformation mechanism is sufficient to reduce the internal stress, σ_i .

A different mechanism for stress-relief cracking in ferritic steels, including the possible effects of impurity elements, has been proposed recently

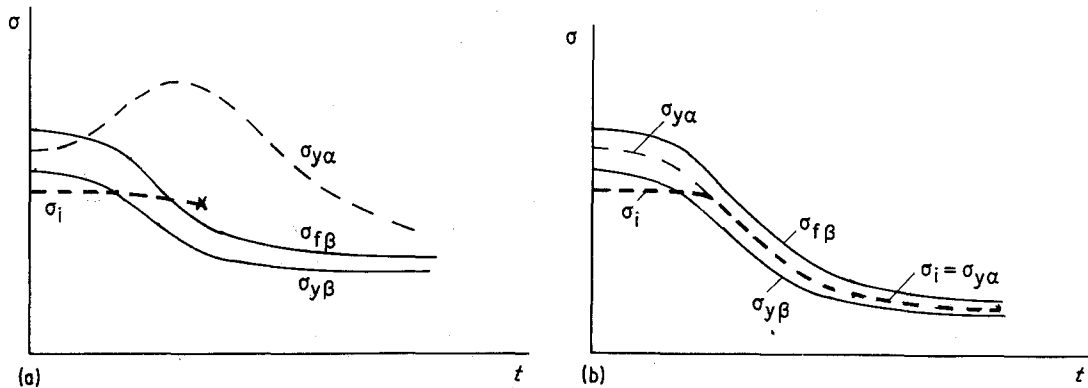


Figure 10 Change of mechanical properties of the grain interior (α) and PFZ (β) during stress-relieving heat-treatment (a) Low alloy steel forming a fine dispersion of alloy carbides within α . (b) Plain carbon steel (σ_i = internal stress; $\sigma_{y\alpha}$ and $\sigma_{y\beta}$ = yield strength of α and PFZ; $\sigma_{f\beta}$ = tensile strength of β).

[34–37]. Cracking was found to result from nucleation and the growth of intergranular cavities in which voids appeared to nucleate on sulphide or carbide particles. The rate of both nucleation and growth of the cavities can be accelerated by segregation of elements like phosphorous, sulphur, nitrogen, tin, antimony and copper to the particle–matrix interface and to the free surface of the cavities.

3.4. Ways to reduce or inhibit pseudo-intercrystalline brittleness

The effect of a PFZ is the more deleterious on elongation at fracture and fracture toughness, (a) the smaller is the diameter of the PFZ, (b) the lower is the tensile strength in the PFZ, (c) the smaller the deformation at fracture in the PFZ, (d) the larger the grain size, and (e) the larger the ratio $\bar{\sigma}_{y\alpha}/\bar{\sigma}_{f\beta}$.

Measures against pseudo-intercrystalline brittleness can be based on a favourable modification of any of these parameters. However in many cases the formation of a PFZ is unavoidable during a heat-treatment or in service at elevated temperature.

(a) The PFZ of Type I can be modified by the temperature of homogenization and cooling rate as it controls the average diffusion paths of vacancies [14, 25].

(b) The formation of a PFZ can sometimes be avoided by dislocation nucleation of particles in the neighbourhood of grain boundaries. This requires a moderate amount of plastic deformation before the precipitation heat-treatment.

(c) The deformation at fracture in the PFZ is lowered by an increasing local volume portion of large non-coherent particles [7, 22], which therefore should be avoided.

(d) The grain size should be as small as possible.

(e) Very strong hardening of the grain interior will be useless, if it does not participate in plastic deformation either in the bulk or at the tip of the crack.

Measures used to reduce the susceptibility of SRC include

(i) modifying the alloy composition, e.g. for pressure vessels the steel 22NiMoCr37 has been replaced by the steel 20MnMoNi55 which has a lower Mo and V content to reduce $\bar{\sigma}_{y\alpha}/\bar{\sigma}_{f\beta}$.

(ii) using multiple layer welding procedures, so that the coarse grained area of the heat-affected zone of each layer gets grain refined during the deposit of the following layer.

(iii) welding with limited heat input, so that the volume-fraction of alloy carbides dissolved during the welding cycle is reduced (reducing $\bar{\sigma}_{y\alpha}/\bar{\sigma}_{f\beta}$).

(iv) using a suitable design of the weldment to avoid stress raisers or using electrodes with the lowest yield strength practicable (lower residual stress).

References

1. C. J. McMAHON, in "Grain Boundaries in Engineering Materials", Proceedings of the 4th Bolton Landing Conference, 1974 edited by J. L. Walters.
2. K. WELPMANN, G. LÜTJERING and W. BUNK, *Aluminium* **50** (1974) 263.
3. J. D. EVENSEN, N. RYUM and J. D. EMBURY, *Mater. Sci. Eng.* **18** (1975) p. 221.
4. J. S. SANTNER and M. E. FINE, *Met. Trans.* **7A** (1976) 601.
5. M. GRÄF and E. HORNBOKEN, *Acta Met.* **25** (1977) 883.
6. E. HORNBOKEN, *Z. Metallkd.* **66** (1975) 511.
7. E. HORNBOKEN and M. GRÄF, *Acta Met.* **25** (1977) 877.
8. R. W. NICHOLS, *Weld. World* **7** (1969) 244.
9. J. D. MURRAY, *Brit. Weld. J.* **14** (1967) 447.
10. L. E. EMMER, C. D. CLAUSER and J. R. LOW, *WRC Bulletin* **183** (1973).
11. R. N. YOUNGER and R. G. BAKER, *Brit. Weld. J.* **8** (1961) 579.
12. D. McKEOWN, *Weld. J. Res. Suppl.* **50** (1971) 201s.
13. U. BRUCH and E. HORNBOKEN, *Arch Eisenhüttenwes.* **49** (1978) 409.
14. G. THOMAS and J. NUTTING, *J. Inst. Met.* **88** (1959/60) 81.
15. A. SAULNIER, *Mem. Sci. Rev. Met.* **58** (1961) 615.
16. H. S. ROSENBAUM and D. TURNBULL, *Acta Met.* **7** (1959) 604.
17. H. S. ROSEMBAUM, D. TURNBULL and E. I. ALESSANDRINI, *ibid.* **7** (1959) 678.
18. A. KELLY and R. B. NICHOLSON, "Precipitation Hardening" (Pergamon Press, Oxford 1963) p. 214.
19. N. RYUM, B. HAEGLAND and T. LINDTVIET, *Z. Metallkd.* **68** (1967) 28.
20. E. HORNBOKEN, in "Nucleation" edited by A. C. Zettlemoyer (Marcel Dekker, New York, 1969) p. 309.
21. M. RAGHAVAN, *Met. Trans.* **11A** (1980) 993.
22. L. M. BROWN and J. D. EMBURY, in "The Microstructure and Design of Alloys", the Proceedings of the 3rd International Conference on the Strength of Metals and Alloys, Cambridge, August 1973 Vol. 1, (The Institute of Metals, London, 1973) p. 164.
23. E. HORNBOKEN and K. FRIEDRICH, *J. Mater. Sci.* **15** (1980) 2175.
24. H. R. TIPLER *et al.*, *Met. Technol.* **2** (1975) 206.
25. U. BRENNER, Ph.D. Thesis University of Bochum 1977.
26. K. B. BENTLEY, *Brit. Weld. J.* **11** (1964) 507.
27. C. F. MEITZNER, *Weld. J. Res. Suppl.* **48** (1969) 431s.

28. H. NAKAMURA, T. NAIKI and H. OKABAYASHI, *J. Jap. Weld. Soc.* **32** (1963) 125.
29. K. DETERT, R. BANGA and W. BERTRAM, *Arch Eisenhüttenwes.* **45** (1974) 245.
30. H. GORETZKI and E. DE LAMOTTE, Proceedings of the Workshop held at the Westinghouse Research Laboratory, Brussels, January 1974 (Westinghouse Corp., Brussels, 1974).
31. H. KREYE, I. OLEFJORD and J. LÖTTGERS, *Arch. Eisenhüttenwes.* **48** (1977) 291.
32. U. BRENNER, H. KREYE and H. BAUMGARDT, *ibid.* **51** (1980) 393.
33. A. G. VINCKIER, Doc. IIW X-750-74, Budapest 1974.
34. C. J. McMAHON, R. J. DOBBS and D. H. GENTNER, *Mater. Sci. Eng.* **37** (1979) 179.
35. C. L. BRIANT and S. K. BANERJI, *Int. Met. Rev.* **23** (1978) 164.
36. C. A. HIPPSLEY, J. F. KNOTT and B. C. EDWARDS, *Acta Met.* **28** (1980) 869.
37. C. A. HIPPSLEY, *Met. Sci.* **15** (1981) 137.

*Received 20 May
and accepted 18 August 1981*